Interactions of Divalent Cations with Phosphatidylserine Bilayer Membranes†

Helmut Hauser and G. Graham Shipley*

ABSTRACT: The interaction of divalent cations with a homologous series of diacylphosphatidylserines (diacyl-PS) has been studied by differential scanning calorimetry and X-ray diffraction. Hydrated di-C_{14}-PS (DMPS) exhibits a gel → liquid-crystal bilayer transition at 39 °C (ΔH = 7.2 kcal/mol of DMPS). With increasing $MgCl_2$ concentration, progressive conversion to a phase exhibiting a high melting (98 °C), high enthalpy ($\Delta H \simeq$ 11.0 kcal/mol of DMPS) transition is observed. Similar behavior is observed for DMPS with increasing $CaCl_2$ concentration. In this case, the high-temperature transition of the Ca^{2+}–DMPS complex occurs at ~155 °C and is immediately followed by an exothermic transition probably associated with PS decomposition. For di-C_{12}-, di-C_{14}-, di-C_{16}- (DPPS), and di-C_{18}-PS, the transition temperatures of the Ca^{2+}–PS complexes are in the range 151–155 °C; only di-C_{10}-PS exhibits a significantly lower value, 142 °C. A different pattern of behavior is exhibited by DPPS in the presence of Sr^{2+} or Ba^{2+}, with transitions in the range 70–80 °C being observed. X-ray diffraction of the Ca^{2+}–PS complexes at 20 °C provides evidence of structural homology. All Ca^{2+}–PS complexes exhibit bilayer structures, the bilayer periodicity increasing linearly from 35.0 Å for di-C_{10}-PS to 52.5 Å for di-C_{18}-PS. Wide-angle X-ray diffraction data indicate that hydrocarbon chain "crystallization" occurs on Ca^{2+}–PS complex formation. Mg^{2+}–DPPS and Ca^{2+}–DPPS form similar ordered bilayer structures (periodicity $d \simeq$ 47–48 Å), but the Sr^{2+}- and Ba^{2+}–DPPS complexes have a larger periodicity ($d \simeq$ 57–58 Å) and a less ordered chain packing mode. Comparison with anhydrous/hydrated PS and M^+–PS complexes allows the structures of the different M^{2+}–PS complexes to be analyzed.

Phosphatidylserine (PS)[1] is the predominant anionic phospholipid in most mammalian cell membranes (Rouser et al., 1968; White, 1973). It is particularly prevalent in peripheral and central nervous system myelin, blood erythrocytes and platelets, and retinal rod outer segment disk membranes, with apparently a preferential distribution on the cytoplasmic side of the membrane bilayer (Verkleij et al., 1973; Schick et al., 1976; Smith et al., 1977). Due to its anionic character at physiological pH, the interactions of PS with biologically important cations have been implicated in membrane-associated events such as membrane fusion (Papahadjopoulos, 1978), lipid phase separation (Ohnishi & Ito, 1974), blood clotting factor binding (Papahadjopoulos & Hanahan, 1964), etc. Thus, the binding of mono- and divalent cations to monolayer and bilayer membranes of PS, usually isolated from bovine brain, has been studied extensively by a variety of biophysical and biochemical methods (Abramson et al., 1964; Papahadjopoulos & Miller, 1967; Atkinson et al., 1974; Hauser & Phillips, 1973; Hope & Cullis, 1980; Ohki & Kurland, 1981; Eisenberg et al., 1979; McLaughlin et al., 1981; Puskin, 1977; Ohki et al., 1982; McLaughlin, 1982; Loosley-Millman et al., 1982; Hauser et al., 1977). Of particular note is the observation by Papahadjopoulos and colleagues that isothermal changes in the state of the PS bilayers are induced by Ca^{2+} binding, domains of high-melting Ca^{2+}–PS complexes being formed (Papahadjopoulos et al., 1977, 1978; Jacobson & Papahadjopoulos, 1975; Newton et al., 1978). It is suggested that interbilayer Ca^{2+}–PS complexes may provide the initial "trigger" for membrane fusion processes [for a review, see Papahadjopoulos (1978)].

Until recently, most physical studies of PS were restricted to heterogeneous, mixed fatty acyl chain PS isolated from bovine brain. Thus, only limited information on PS structure, properties, and interactions has been available. The availability of chemically defined, synthetic PS with controlled fatty acyl chain composition has led to a better understanding of the thermotropic properties of PS and its ion binding properties. DPPS, for example, undergoes a bilayer gel to liquid-crystal transition at ~53 °C as demonstrated by differential scanning calorimetry (MacDonald et al., 1976; van Dijck et al., 1978; Browning & Seelig, 1980; Cevc et al., 1981; Hauser et al., 1982), spin-label partitioning (Luna & McConnell, 1977; Cevc et al., 1981), and ^{31}P and ^{2}H nuclear magnetic resonance (Browning & Seelig, 1980). In a scanning calorimetry study, van Dijck et al. (1978) demonstrated that the transition temperature of DMPS was dependent on the charge of the carboxylate group. A more extensive study of the pH dependence of the transition behavior of DMPS and DPPS utilizing DSC and spin-label/electron-spin resonance confirms this behavior and identifies a second pK_a corresponding to deprotonation of the amino group of the serine moiety (Cevc et al., 1981). These authors also studied in detail the effect of Na^+ concentration on DMPS phase transitions. Na^+ concentrations in the range 0–2.0 M increased the phase transition temperature of DMPS by ~6 °C; a somewhat larger increase in the transition temperature was observed in the range 2.0–6 M NaCl.

Our own studies have examined the structure and thermotropic properties of a homologous series of synthetic diacyl-PS (di-$C_{10:0}$, di-$C_{12:0}$, di-$C_{14:0}$, di-$C_{16:0}$, and di-$C_{18:0}$) in the presence and absence of monovalent cations (Hauser et al., 1982; Hauser & Shipley, 1983). Using DSC and X-ray diffraction, these synthetic PS were shown to form "continuously" hydrated

† From the Biophysics Division, Departments of Medicine and Biochemistry, Boston University School of Medicine, Boston, Massachusetts 02118. *Received May 11, 1983; revised manuscript received August 22, 1983.* This research was supported by research grants from the National Institutes of Health (HL-26335) and the Swiss National Science Foundation (3.156-0.81). H.H. was on sabbatical leave from the Biochemistry Department, ETH-Zurich, Switzerland, and was supported by a short-term fellowship from the European Molecular Biology Organization and by the Zentenarfond (ETH-Zurich).

[1] Abbreviations: PS, phosphatidylserine(s); DDPS, didecanoylphosphatidylserine; DLPS, dilauroylphosphatidylserine; DMPS, dimyristoylphosphatidylserine; DPPS, dipalmitoylphosphatidylserine; DSPS, distearoylphosphatidylserine; DSC, differential scanning calorimetry; TLC, thin-layer chromatography.

0006-2960/84/0423-0034$01.50/0

bilayer structures exhibiting chain length dependent gel → liquid-crystal transitions (Hauser et al., 1982). Again, only small increases in the transition temperature were observed for PS dispersed in up to 1.5 M sodium chloride (and other alkali metal chlorides) [Hauser & Shipley, 1983; see also Cevc et al. (1981)], the major effect being a decrease in bilayer periodicity as Na^+ ions shield the negatively charged bilayer surface. The thickness of the aqueous compartment is reduced without significant changes in the structure of the PS bilayer itself (Hauser & Shipley, 1983). In contrast, LiCl produces "crystallization" and dehydration of PS bilayers, with the Li^+–PS complexes exhibiting bilayer gel → liquid-crystal transitions at much higher temperatures (Hauser & Shipley, 1981, 1983). This behavior is reminiscent of the effect of divalent cations such as Ca^{2+} and Mg^{2+} on bovine brain PS bilayers.

The study reported here documents the major changes in structure and thermotropic properties of the same homologous series of PS (di-C_{10} to di-C_{18}) induced by Mg^{2+}, Ca^{2+}, Sr^{2+}, and Ba^{2+} and allows a detailed comparison of the differing effects of monovalent and divalent cations on PS bilayers.

Materials and Methods

Materials

A homologous series of 2,3-diacyl-D-glycero-1-phospho-L-serines [for a discussion of the chemical nomenclature used, see Hauser et al. (1981)] was synthesized as described elsewhere (Hermetter et al., 1982). The acid form of phosphatidylserine was converted into the ammonium salt, and the purity of the lipid was monitored by TLC as described previously (Hauser et al., 1982).

Sample Preparation. Unless otherwise stated, hydrated samples of NH_4^+–DMPS for DSC analysis were prepared by weighing a known amount of the lipid into the DSC pan and by injecting the appropriate amount of water or divalent cation salt solution. The DSC pan was immediately sealed and transferred to the scanning calorimeter. For X-ray diffraction studies, the divalent cation salts of different phosphatidylserines were prepared by weighing a known amount of the NH_4^+ salt of PS into a glass tube with a narrow constriction in the center and adding an excess of the divalent metal chloride solution. The glass tube was immediately sealed and the lipid dispersion homogenized by centrifuging through the narrow constriction repeatedly (6–12 times) at a temperature above the chain melting transition. Some samples prepared according to this method were examined by both X-ray diffraction and DSC. In some instances, the Ca^{2+} salts of phosphatidylserines formed as described above were dried to constant weight under vacuum. Alternatively, the Ca^{2+} salt was dispersed in acetone and the dispersion filtered through a glass-sintered disk. This procedure was repeated 3–6 times to remove excess H_2O. The Ca^{2+} salts thus treated were dried to constant weight under vacuum.

Alternatively, the metal ion salts of DPPS were prepared from sonicated lipid dispersions (~1% ≃ 10 mM) by precipitation with an excess of metal ion (~>0.5 M). The molar ratio *total* metal ion:DPPS was ~50:1. Unsonicated dispersions of NH_4^+–DPPS were prepared by drying the lipid from a chloroform/methanol solution (2:1 v/v) in a rotary evaporator, and further drying the lipid under vacuum. To the dry lipid (~30 mg) was added 3 mL of 0.015 M ammonium phosphate buffer, pH 6.9, at a temperature slightly above the transition temperature (T_c), and the lipid was dispersed by vortexing at this temperature. The lipid dispersion was flushed with nitrogen and sonicated at a temperature greater than the T_c with a Branson sonifier using a microtip (50% duty cycle). After sonication, the sample was centrifuged at 5000 rpm to remove any titanium released from the tip of the probe.

Methods

Calorimetric studies were performed with a Perkin-Elmer (Norwalk, CT) DSC-2 differential scanning calorimeter. Samples were heated and cooled repeatedly, usually at a rate of 5 °C/min. The peak in the heat capacity vs. temperature plot was taken as the transition temperature. Transition enthalpies were determined from the area under the peak as measured by planimetry and standardized against gallium and indium.

For X-ray diffraction studies, nickel-filtered Cu Kα X radiation from an Elliot GX-6 rotating anode generator (Elliott Automation, Borehamwood, England) was used. The X-rays were focused by using a camera with toroidal optics (Elliott, 1951), and the X-ray diffraction patterns were recorded from samples maintained at different temperatures by utilizing a variable temperature specimen holder.

Results

Differential Scanning Calorimetry. The NH_4^+ salt of DMPS dispersed in excess 0.15 M NaCl, pH 6.5, gave reproducible, sharp order–disorder transitions on both heating (Figure 1A) and cooling. On heating, the endothermic transition was at 39 °C (ΔH = 7.2 kcal/mol of DMPS), and upon cooling, the transition was depressed by ~4 °C. The addition of $MgCl_2$ had no detectable effect on the thermotropic behavior of DMPS up to [$MgCl_2$] ≃ 1 mM. Above this concentration, additional endothermic transitions were observed. At ≃8 mM $MgCl_2$, corresponding to a molar ratio Mg^{2+}(total):DMPS = 0.15, the major transition at 39 °C is followed by a low-enthalpy endotherm at 48 °C (Figure 1B). At 16 mM $MgCl_2$, Mg^{2+}(total):DMPS = 0.34, an additional broad transition centered at about 92 °C is observed (Figure 1C). The temperature of the latter transition increased progressively with increasing $MgCl_2$ concentration (Figure 1C–G), reaching a maximum of 98 °C at 1 M $MgCl_2$, Mg^{2+}(total):DMPS = 31.6 (Figure 1G). Clearly, up to three transitions are detectable at low $MgCl_2$ concentrations (see, for example, Figure 1C). The transition temperatures of the two lower transitions (shown in Figure 1B,C) increase slightly with increasing $MgCl_2$ concentration (data not shown). The transition enthalpy associated with the peak at ~92 °C increases, and concomitantly, the enthalpies associated with the two low-temperature transitions decrease. At [$MgCl_2$] ≃ 20 mM, Mg^{2+}(total):DMPS = 0.61, the two low-temperature transitions are barely detectable (Figure 1D), and at higher $MgCl_2$ concentrations, they have disappeared completely (Figure 1E–G). The enthalpy, ΔH, for the high-temperature transition for aqueous NH_4^+–DMPS dispersions was invariant over the range [$MgCl_2$] = 80 mM [Mg^{2+}(total):DMPS = 1.74] to 1 M [Mg^{2+}(total):DMPS = 31.6]. The ΔH value obtained for this concentration range is 11.0 ± 1.6 kcal/mol of DMPS.

The effect of $CaCl_2$ concentration on the thermal behavior of NH_4^+–DMPS dispersions in excess 0.15 M NaCl, pH 6.5, is shown in Figure 2. The effect of $CaCl_2$ concentration is qualitatively similar to that of $MgCl_2$. Effects on the thermotropic behavior of NH_4^+–DMPS dispersions in 0.15 M NaCl were detectable only at [$CaCl_2$] > 1 mM. At [$CaCl_2$] of 8 mM [Ca^{2+}(total):DMPS = 0.27] and 20 mM [Ca^{2+}(total):DMPS = 0.44], a small transition appeared between 44 and 50 °C (Figure 2B,C), in addition to the transition at ~40 °C characteristic of NH_4^+–DMPS (see Figure 2A). Both of these transitions increase slightly in temperature with in-

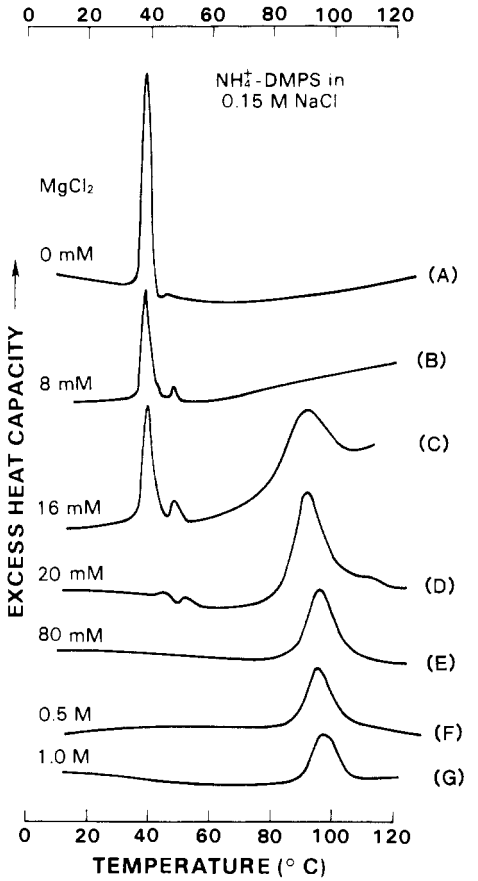

FIGURE 1: (A) DSC heating curve of NH_4^+–DMPS (43.0 mM = ~3 wt %) dispersed in 0.15 M NaCl, pH 6.5. Upon cooling, a single sharp transition occurred, the temperature of which was depressed by 4–6 °C compared to the heating curve. (B–G) DSC heating curves of NH_4^+–DMPS dispersed in 0.15 M NaCl, pH 6.5, as a function of $MgCl_2$ concentration. Heating curves are shown for 8 mM $MgCl_2$, NH_4^+–DMPS = 54.5 mM (3.8%), molar ratio Mg^{2+}(total):DMPS = 0.15 (B); 16 mM $MgCl_2$, NH_4^+–DMPS = 47.4 mM (3.3%), Mg^{2+}(total):DMPS = 0.34 (C); 20 mM $MgCl_2$, NH_4^+–DMPS = 33.0 mM (2.3%), Mg^{2+}(total):DMPS = 0.61 (D); 80 mM $MgCl_2$, NH_4^+–DMPS = 45.9 mM (3.2%), Mg^{2+}(total):DMPS = 1.74 (E); 0.5 M $MgCl_2$, NH_4^+–DMPS = 68.9 mM (4.8%), Mg^{2+}(total):DMPS = 7.26 (F); and 1 M $MgCl_2$, NH_4^+–DMPS = 31.6 mM (2.2%), Mg^{2+}(total):DMPS = 31.6 (G). Heating rate = 5 °C/min.

creasing $CaCl_2$ concentration (data not shown). At [$CaCl_2$] >20 mM, corresponding to Ca^{2+}(total):DMPS > 0.44, a broad, asymmetric endothermic peak was observed at temperatures >154 °C (Figure 2C and Figure 3C) which can be assigned to the Ca^{2+} complex of DMPS. This broad endotherm is immediately followed by an exothermic peak. The high-temperature transition is irreversible; upon cooling the sample to 4 °C and reheating, a single endothermic transition was obtained at 51.5 °C, but no endothermic transition was observed at higher temperatures. The thermal behavior of a sample treated in this way was reproducible on successive heating–cooling cycles. However, examination by TLC of the sample after heating to temperatures >155 °C showed that DMPS had undergone significant chemical decomposition by this treatment; the nature of the degradation products was not investigated.

As observed with $MgCl_2$, with increasing $CaCl_2$ concentration, the total enthalpy of the low-temperature transitions decreased as that of the broad asymmetric transition at high temperature (~155 °C) increased. The presence of the exotherm following the high-temperature endothermic transition of the Ca^{2+}–DMPS complex prohibits an accurate measurement of the peak area and hence of ΔH for the Ca^{2+}–DMPS

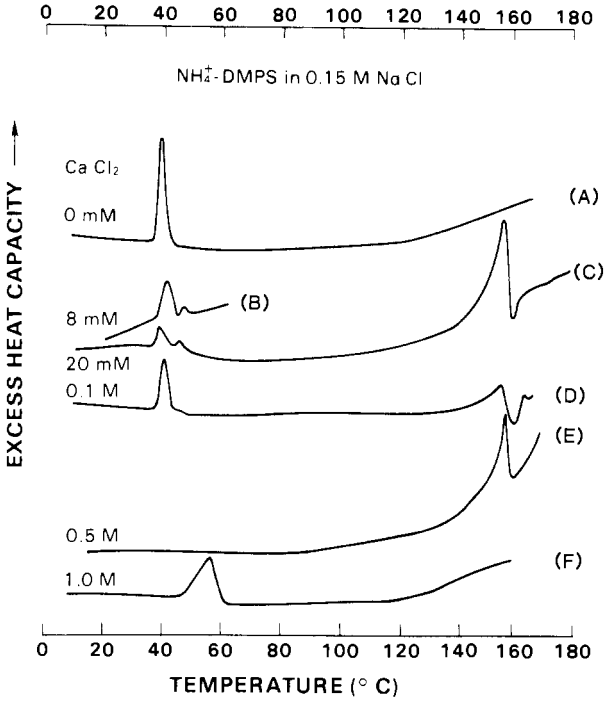

FIGURE 2: (A) DSC heating curve of NH_4^+–DMPS (43.0 mM ≃ 3 wt %) dispersed in 0.15 M NaCl, pH 6.5; the transition temperature of the cooling curve was depressed by ~5 °C. (B–F) DSC heating curves of NH_4^+–DMPS dispersed in 0.15 M NaCl, pH 6.5, as a function of $CaCl_2$ concentration. Heating curves are shown for 8 mM $CaCl_2$, NH_4^+–DMPS = 29.7 mM (2%), molar ratio Ca^{2+}(total):DMPS = 0.27 (B); 20 mM $CaCl_2$, NH_4^+–DMPS = 45.9 mM (3.2%), Ca^{2+}(total):DMPS = 0.44 (C); 0.1 M $CaCl_2$, NH_4^+–DMPS = 51.7 mM (3.6%), Ca^{2+}(total):DMPS = 1.93 (D); 0.5 M $CaCl_2$, NH_4^+–DMPS = 23 mM (1.6%), Ca^{2+}(total):DMPS = 21.7 (E); and 1 M $CaCl_2$, NH_4^+–DMPS 36.2 mM (2.5%), Ca^{2+}(total):DMPS = 27.6 (F). Heating rate = 5 °C/min.

melting transition. Attempts to calculate ΔH for the Ca^{2+}–DMPS complex produced low values (6.3 kcal/mol of DMPS) compared to that of the Mg^{2+} complex (11.0 kcal/mol of DMPS). Sometimes in samples of NH_4^+–DMPS containing 0.5 M $CaCl_2$, a low-temperature transition at 40–45 °C was observed in addition to that at high temperature.

The thermal behavior of NH_4^+–DMPS in the presence of 1 M $CaCl_2$, $CaCl_2$(total):DMPS = 27.6, differs from that observed at lower $CaCl_2$ concentrations. A single, relatively broad transition was observed reproducibly between 47 and 56 °C with no further endothermic transition up to ~170 °C (Figure 2F). This suggests that under these conditions Ca^{2+} forms a different phase with DMPS from that present at lower $CaCl_2$ concentrations. The DSC heating curve of an NH_4^+–DPPS sample in the presence of 1 M $CaCl_2$, Ca^{2+}-(total):DPPS = 14.3, shows a transition at low temperature (~64 °C; data not shown) which is about 10–17 °C higher than the corresponding DMPS–Ca^{2+} transition. In contrast to DMPS, there is some evidence of another transition at 158 °C, indicating that the high-melting Ca^{2+}–DPPS complex is at least partially formed in the presence of 1 M $CaCl_2$.

The other members of the homologous series of saturated phosphatidylserines (di-C_{10}–di-C_{18}) interact with Ca^{2+} in a fashion similar to but not identical with NH_4^+–DMPS. In the presence or absence of NaCl, Ca^{2+} (0.5–1 M $CaCl_2$) formed high-melting complexes with all phosphatidylserines investigated. These Ca^{2+}–PS complexes gave broad endothermic transitions at temperatures between 142 and 157 °C (Figure 3). As discussed above for NH_4^+–DMPS, the endothermic transition at temperatures >140 °C was immediately followed by an exothermic one. Again, for all phosphati-

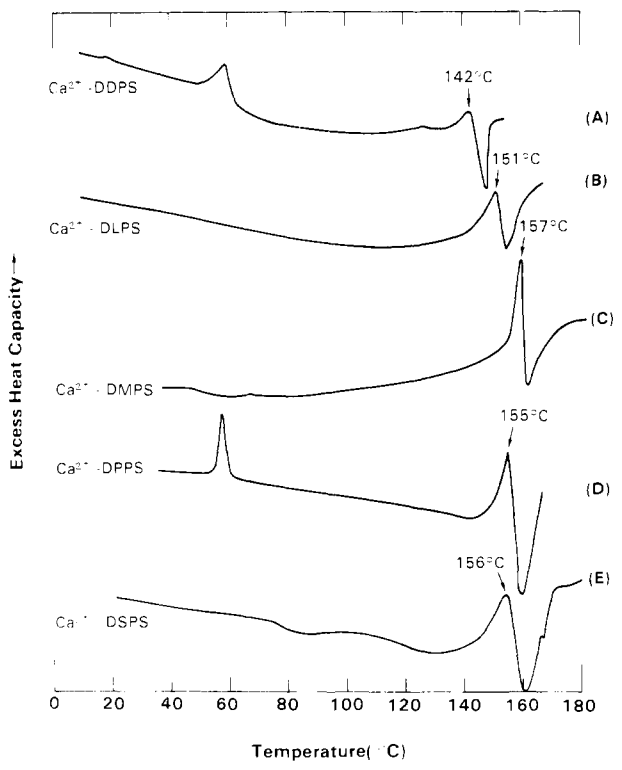

FIGURE 3: DSC heating curves of the Ca^{2+} complexes of different phosphatidylserines. Except for the Ca^{2+}–DPPS complex, the Ca^{2+} complexes were prepared by equilibrating the lipid with a 0.5 M $CaCl_2$ solution in the constricted sample tube as described under Methods. The Ca^{2+} complex of DPPS was prepared by weighing the lipid into the DSC pan and adding the appropriate amount of 0.5 M $CaCl_2$. Heating curves were recorded at 5 °C/min and are shown for the Ca^{2+} complexes of DDPS (~0.5 M ≃ 30%), molar ratio Ca^{2+}(total):DDPS = 1.0 (A); DLPS (~0.2 M ≃ 13%), Ca^{2+}(total):DLPS = 2.5 (B); DMPS (~0.24 M ≃ 17%), Ca^{2+}(total):DMPS = 2.0 (C); DPPS (~0.048 M ≃ 3.6%), Ca^{2+}(total):DPPS = 10.0 (D); and DSPS (~0.25 M ≃ 20%), Ca^{2+}(total):DSPS = 2.0 (E).

dylserines studied, the high-temperature transition was irreversible; i.e., it was not observed when the heating–cooling cycle was repeated. For DDPS and DPPS, an additional low-temperature transition at ~58–59 °C was observed. For DDPS (see Figure 3A), the ratio Ca^{2+}:DDPS was 1.0, and *possibly* insufficient Ca^{2+} ions were present for complete conversion to the high-temperature form. This would not appear to be the explanation for DPPS (Figure 3D), where the Ca^{2+} ion is present in a 10-fold excess over DPPS (see also Figure 2F for similar behavior of Ca^{2+}–DMPS).

The transition temperature of the Ca^{2+}–PS complexes is apparently chain length independent. Only DDPS gave a Ca^{2+} complex with a transition temperature significantly lower than 150 °C. All other Ca^{2+}–PS complexes gave transitions between 150 and 160 °C.

Drying the Ca^{2+}–PS complexes to constant weight as described under Materials and Methods had different effects. The dried Ca^{2+} complexes of DLPS and DMPS gave broad transitions which occurred at lower temperatures compared to the Ca^{2+}–PS complexes dispersed in excess aqueous buffer (data not shown). In both cases, the broad transition consisted of a relatively sharp peak at 125 °C for DLPS and at 127 °C for DMPS followed by a broad shoulder at ~130 °C for DLPS and at ~140 °C for DMPS. This behavior is contrasted by the dried Ca^{2+}–PS complex of DSPS which gave a single broad transition at ~186 °C, more than 30 °C higher than that of the Ca^{2+} complex of DSPS in excess aqueous buffer. No other transition was detectable at lower temperatures.

DSC thermograms of unsonicated and sonicated DPPS dispersed in 0.025 M phosphate buffer, pH 6.8, are shown in parts A and B, respectively, of Figure 4. Both unsonicated and sonicated dispersions gave reproducible, sharp order–disorder transitions on heating. Surprisingly, the transition temperature of sonicated phosphatidylserine dispersions (57 °C) was a few degrees *higher* than that of the corresponding unsonicated dispersion (53 °C). Upon cooling unsonicated DPPS, a single sharp transition was observed reproducibly which was depressed by about 5 °C. This is contrasted by the behavior of sonicated DPPS dispersions in the same aqueous buffer. In this case, a broad transition is obtained, also reproducibly, which consists of at least three peaks. The temperature of the main transition is lowered by ~8 °C.

The DSC heating curves of sonicated DPPS after the addition of a 50 molar excess of Ca^{2+}, Sr^{2+}, and Ba^{2+} are shown in Figure 4C. For comparison, the DSC heating curve of the complex formed between sonicated DPPS and excess Li^+ is also included. The transition temperatures of the Ca^{2+} and Li^+ complexes formed from sonicated DPPS complexes are similar to those formed from unsonicated DPPS dispersions [see above and Hauser & Shipley (1983)], indicating that the metal ion–PS complex formed is independent of the state of the starting dispersion. The complex of DPPS with Sr^{2+} shows evidence of a transition at ~155 °C, similar to that of the Ca^{2+} complex (~156 °C), while the Ba^{2+} complex shows a broad endotherm at ~174 °C, significantly higher than that of the other complexes. While the Li^+ and Ca^{2+} complexes gave single endothermic transitions at 95 and 156 °C, respectively, the other metal ions gave rise to a more complex thermal behavior; in addition to the high-temperature transition, a transition at low temperatures (70–80 °C) was observed in the presence of Sr^{2+} and Ba^{2+}.

X-ray Diffraction. X-ray diffraction patterns of the homologous series di-C_{10}–di-C_{18} of NH_4^+–PS following precipitation by excess $CaCl_2$ were recorded at 20 °C, and examples are shown in Figure 5. There is clear evidence that all of the complexes produced are lamellar and isostructural. First, the diffraction lines in the range 1/3.0 to 1/5.0 $Å^{-1}$ are similar for all chain lengths. Second, a strong reflection characteristic of this structural form is present at 1/8.0 $Å^{-1}$. Finally, a plot of the lamellar periodicity vs. chain length is linear (Figure 7). From the slope, an increment of 2.0 Å per CH_2 group is derived, and the extrapolation to zero chain length indicates a contribution of 14 Å from two glycerophosphoserine head groups. It should be noted that this chain-length dependence of the bilayer periodicity is similar to that of one of the anhydrous forms of PS [type II; see Hauser et al. (1982)]. These data suggest that Ca^{2+} interacts with PS in a chain length independent fashion to produce "crystalline" Ca^{2+}–PS bilayers with an ordered hydrocarbon chain packing mode.

In addition, the precipitate formed when Ca^{2+} (0.5 M) was added to a sonicated dispersion of NH_4^+–DPPS (1% ≃ 0.013 M) was studied by X-ray diffraction. The X-ray diffraction pattern of the Ca^{2+}–DPPS complex was extremely weak, and only a single low-angle reflection corresponding to d = 47 Å was observed. Washing this precipitate with acetone and drying did not have any effect on the X-ray pattern. The d value observed is consistent with the first-order reflection of the lamellar repeat distance of Ca^{2+}–DPPS (50%) prepared from an unsonicated dispersion (see above and Figure 7). Similar observations were made with other alkaline earth metal ions and Li^+, which at a concentration of 0.5 M all precipitate sonicated NH_4^+–DPPS. For sonicated NH_4^+–DMPS, Ca^{2+} and Li^+ also produce precipitation of lamellar complexes [for

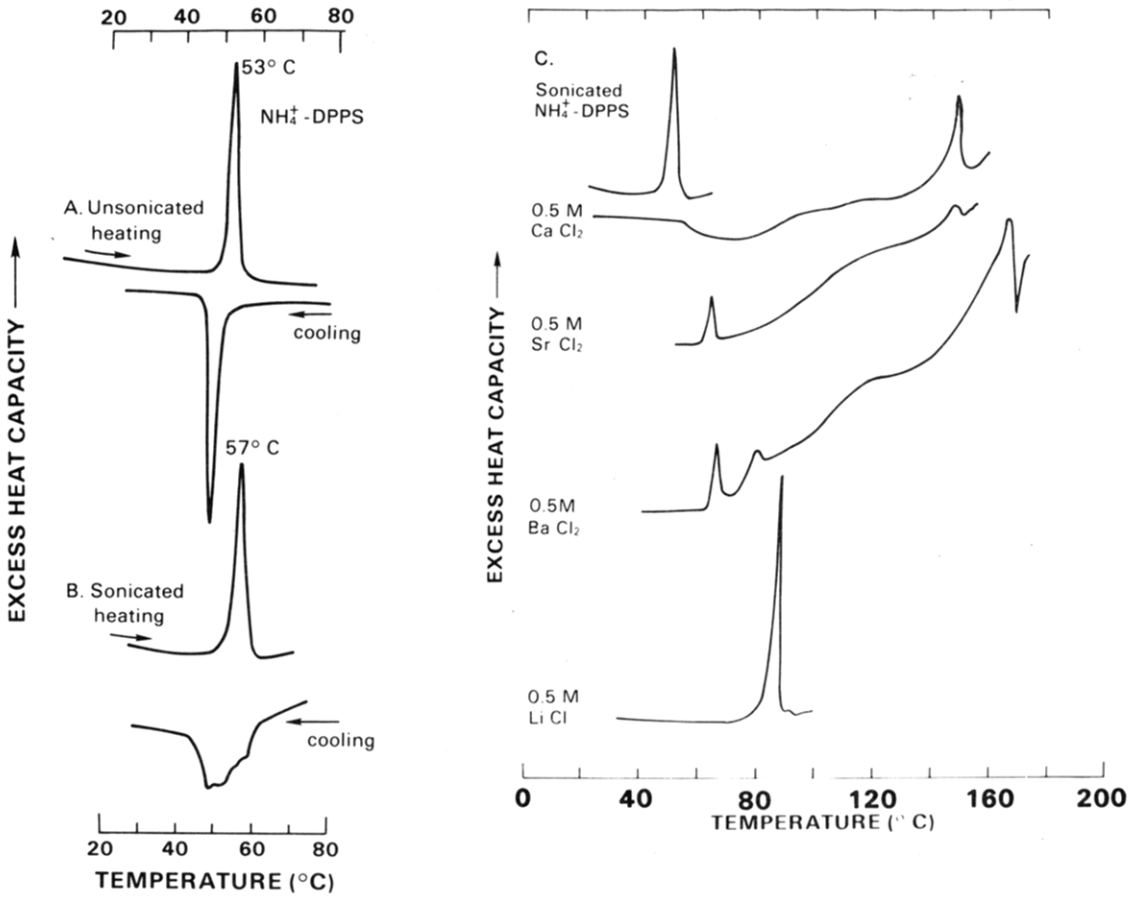

FIGURE 4: (A) DSC heating and cooling curves of unsonicated NH_4^+–DPPS dispersions (0.040 M $\simeq$ 3%) in 0.025 M ammonium phosphate buffer, pH 6.8 (I = 0.05), in the absence of NaCl. (B) DSC heating and cooling curves of sonicated dispersions of NH_4^+–DPPS [same buffer as in (A)]. (C) DSC heating curves of precipitates formed from the sonicated NH_4^+–DPPS dispersion by adding a 50 molar excess of $CaCl_2$, $SrCl_2$, and $BaCl_2$. The precipitates were formed by injecting 30 μL of the sonicated NH_4^+–DPPS dispersion into the DSC pan and by adding the same volume of a 1 M solution of the corresponding metal ion solution; the M^{2+}(total):DPPS molar ratio equals 50.0. For comparison, the DSC heating curve of sonicated NH_4^+–DPPS precipitated by LiCl is shown. One milliliter of the sonicated dispersion of NH_4^+–DPPS described in (B) was diluted with an equal volume of 1 M LiCl. The precipitate was spun down at approximately 5000 rpm and the wet pellet loaded into the DSC pan. The heating rate in all cases was 5 °C/min.

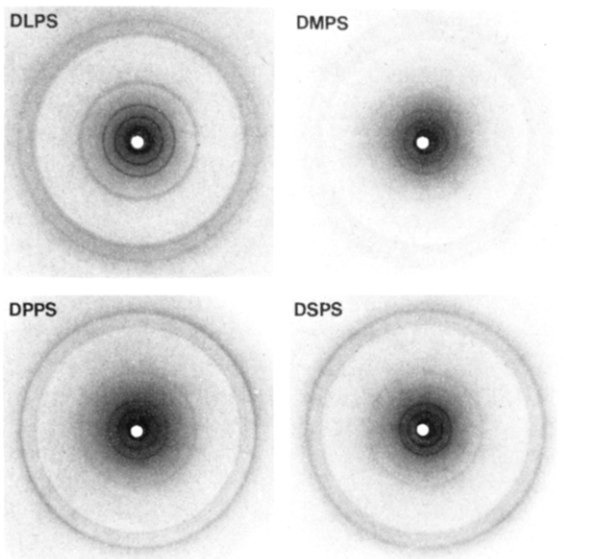

FIGURE 5: X-ray diffraction patterns of Ca^{2+} complexes of different PS: Ca^{2+}–DLPS; Ca^{2+}–DMPS; Ca^{2+}–DPPS; Ca^{2+}–DSPS. X-ray diffraction patterns were recorded at 20 °C on a toroidal camera, sample to film distance = 62.95 mm.

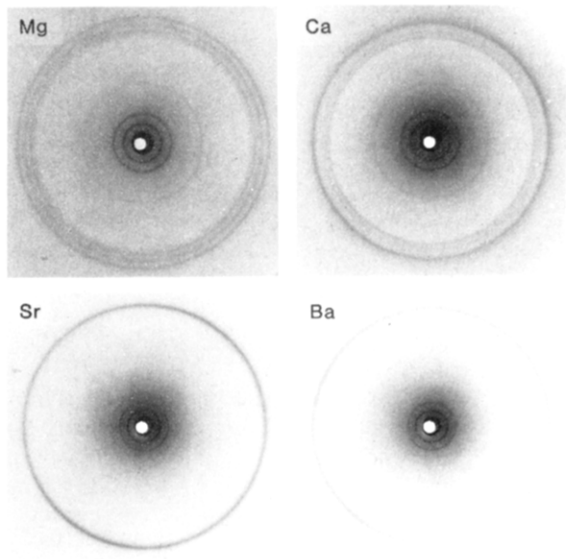

FIGURE 6: X-ray diffraction patterns of M^{2+}–DPPS complexes: Mg^{2+}–DPPS; Ca^{2+}–DPPS; Sr^{2+}–DPPS; Ba^{2+}–DPPS. X-ray diffraction patterns were recorded at 20 °C on a toroidal camera, sample to film distance = 62.95 mm.

Li^+, see Hauser & Shipley (1981, 1983)].

In addition, we have analyzed the interactions of $MgCl_2$ with di-C_{12}–di-C_{18}-PS. In this case, the data are more difficult to rationalize. Mg^{2+}–DMPS and Mg^{2+}–DPPS (see Figure 6) exhibit diffraction patterns similar to but not identical with their Ca^{2+} (cf. Figure 5) and Li^+ counterparts. Again, a

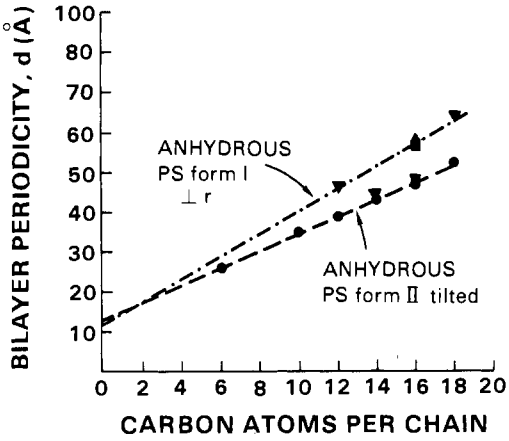

FIGURE 7: Bilayer periodicity as a function of chain length for different M^{2+} salts of PS. The plotted points represent experimental bilayer periodicities derived for (▼) Mg^{2+}, (●) Ca^{2+}, (■) Sr^{2+}, and (▲) Ba^{2+} complexes of PS. The plotted lines represent the regression lines derived from the bilayer periodicities of two different polymorphic forms, I (·····) and II (---), of the anhydrous acidic and salt forms of PS [see Hauser et al. (1982)].

number of sharp diffraction lines are observed in the angular range 1/3.0 to 1/5.0 $Å^{-1}$, as well as a strong reflection at 1/8.0 $Å^{-1}$, indicative of chain crystallization. In addition, the lamellar periodicities of Mg^{2+}–DMPS (44 Å) and Mg^{2+}–DPPS (48 Å) are similar to those of the analogous Ca^{2+} complexes (see Figure 7). Thus, our data suggest that for DMPS and DPPS, crystalline complexes are formed following interaction with either Mg^{2+} or Ca^{2+}. In contrast, Mg^{2+}–DLPS and Mg^{2+}–DSPS appear not to form complexes identical with the other homologues. These Mg^{2+}–PS complexes exhibit only a single sharp diffraction line at 1/4.2 $Å^{-1}$ more typical of the "hexagonal" chain packing mode of gel-phase phospholipids. Furthermore, their lamellar periodicities (48 and 64 Å for Mg^{2+}–DLPS and Mg^{2+}–DSPS, respectively) show no homology with the other Mg^{2+}– and Ca^{2+}–PS complexes (see above). In fact, as shown in Figure 7, the lamellar periodicities of Mg^{2+} complexes of DLPS and DSPS are similar to those exhibited by anhydrous NH_4^+– and K^+–PS, and acidic PS (type I) [see Hauser et al. (1982)]. Thus, it appears that structurally different complexes of Mg^{2+} with PS are observed depending on the chain length of the PS.

Finally, we have examined the interaction of the group 2 metal chlorides ($MgCl_2$, $CaCl_2$, $SrCl_2$, and $BaCl_2$) with DPPS. The X-ray diffraction patterns are shown in Figure 6 and indicate clearly that the lamellar structures formed vary according to the metal ion. As indicated above, the Mg^{2+}– and Ca^{2+}–DPPS complexes are similar. In contrast, the Sr^{2+} and Ba^{2+} complexes of DPPS exhibit different diffraction patterns. For example, Sr^{2+}–DPPS shows only a single sharp reflection at 1/4.2 $Å^{-1}$ while Ba^{2+}–DPPS shows some, albeit weak, additional lines in the angular range 1/3.0 to 1/5.0 $Å^{-1}$. Similar behavior is exhibited by the Pr^{3+}–DPPS complex (data not shown). The bilayer periodicities for Sr^{2+}– and Ba^{2+}–DPPS are similar (see Figure 7) and similar to those of both acidic DPPS (type 1) and the NH_4^+– and K^+–DPPS complexes [see Hauser et al. (1982)]. However, their bilayer periodicity is significantly larger (~10 Å) than that of the corresponding Mg^{2+}– and Ca^{2+}–DPPS complexes (Figure 7).

Discussion

Mg^{2+}–PS Complexes. The calorimetric and X-ray diffraction data show clearly that Mg^{2+} can form high-melting complexes with synthetic diacyl-PS. For DMPS, conversion to the high-melting (98 °C) Mg^{2+}–DMPS complex is complete at a molar ratio Mg^{2+}(total):DMPS = 1.7 (see Figure 1E). At lower Mg^{2+} concentrations, the presence of the two major transitions at ~40 and ~90 °C shows clear evidence for the coexistence of laterally segregated domains of Mg^{2+}-free DMPS and Mg^{2+}-DMPS complex bilayers. The transition of the high-melting Mg^{2+}–DMPS complex is quite broad ($\Delta T \simeq 15$ °C), and the transition enthalpy (ΔH = 11 kcal/mol of DMPS) is significantly higher than that of DMPS in the absence of Mg^{2+} (ΔH = 7.2 kcal/mol of DMPS). The X-ray diffraction data show that formation of the Mg^{2+}–DMPS complex is associated with both increased lateral intermolecular interactions (as indicated by the wide-angle diffraction lines) and decreased bilayer periodicity associated with bilayer dehydration. Thus, for DMPS, the binding of Mg^{2+} ions at the DMPS bilayer interface induces the formation of a highly organized, crystalline dehydrated Mg^{2+}–PS complex. Exactly analogous behavior is exhibited by the Mg^{2+}–DPPS system. As shown in Figure 7, the Mg^{2+}–DMPS and Mg^{2+}–DPPS complexes exhibit bilayer periodicities identical with those of the corresponding *anhydrous* form II PS. From arguments presented previously (Hauser et al., 1982), we suggest that the Mg^{2+}–DMPS and –DPPS complexes have a tilted hydrocarbon chain arrangement (see Figure 8).

Although we do not have detailed calorimetric and X-ray diffraction data for DLPS and DSPS, Mg^{2+} again induces bilayer dehydration. However, the bilayer periodicities for the Mg^{2+}–DLPS and –DSPS complexes lie on the line corresponding to the *anhydrous* form I PS (see Figure 7). Again, on the basis of previous arguments (Hauser et al., 1982), these Mg^{2+}–PS complexes adopt a bilayer arrangement with the hydrocarbon chains packed perpendicular to the plane of the bilayer. In addition, the Mg^{2+}–DLPS and –DSPS complexes exhibit only a single diffraction line at 1/4.2 $Å^{-1}$ in the wide-angle region, and thus, under these conditions at least, chain crystallization does not occur. Further experiments are required in order to understand this unusual chain length dependence exhibited by the Mg^{2+}–PS complexes.

Ca^{2+}–PS Complexes. For DMPS, addition of Ca^{2+} induces the formation of a high-melting (155 °C) Ca^{2+}–DMPS complex. Complete complex formation is achieved between a Ca^{2+}(total):DMPS molar ratio of 2 and 22 (see Figure 2D,E). In 0.5 M $CaCl_2$, Ca^{2+}(total):DMPS = 21.7, only the high-melting Ca^{2+}–DMPS complex is observed (Figure 2E); the transition endotherm at 155 °C is followed immediately by an exotherm, which together with problems associated with base-line curvature makes the transition enthalpy difficult to determine with precision. It should be noted that at 0.5 M $CaCl_2$ all of the DMPS is in the high-melting Ca^{2+}–DMPS form. In contrast, at higher Ca^{2+} concentrations, no high-temperature transition is observed at 155 °C, and a transition is now present at ~55 °C (Figure 2F). Thus, additional Ca^{2+} ions must in some way disrupt the molecular packing associated with the high-melting Ca^{2+}–DMPS complex. Similar behavior is exhibited by DPPS dispersed in 1 M $CaCl_2$.

$CaCl_2$ induces the formation of high-melting complexes for DDPS, DLPS, DMPS, DPPS, and DSPS (see Figure 3). These Ca^{2+}–PS complexes all melt between 142 and 157 °C and in contrast to PS bilayers in the absence of divalent cations do not show a significant chain length dependence of the transition temperature; presumably, the melting process of the Ca^{2+}–PS complex involves a dominant contribution from the melting of the Ca^{2+}–polar group lattice. As indicated above, in all cases, this high-temperature transition is followed immediately by a transition exotherm, and the high-temperature transition is not observed following cooling and reheating.

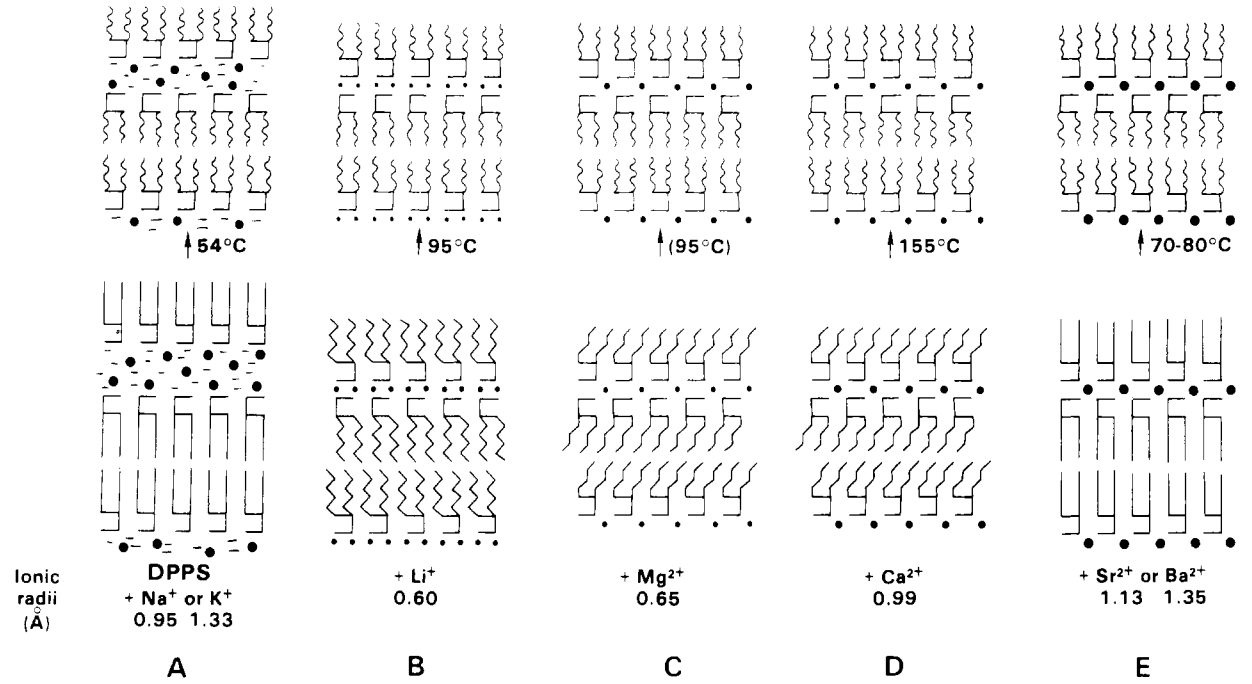

FIGURE 8: Schematic representations of the structures formed by hydrated NH_4^+–DPPS in the presence of Na^+ or K^+ (A), Li^+ (B), Mg^{2+} (C), Ca^{2+} (D), and Sr^{2+} or Ba^{2+} (E). For the hydrocarbon chain region, zigzags represent crystalline chain packing, straight lines represent gel-state chain packing, and wavy lines represent melted chain packing. Solid circles represent cations. It should be noted that the precise molecular arrangements (lamellar, hexagonal, etc.) of the high-temperature forms of the Li^+, Mg^{2+}, Ca^{2+}, Sr^{2+}, and Ba^{2+} complexes are not known.

Although this behavior suggests some complex metastable behavior, problems associated with chemical degradation of PS at these elevated temperatures have precluded a more detailed study of this aspect to the Ca^{2+}–PS interactions. It should also be noted that at a molar ratio Ca^{2+}:DPPS = 10 an additional low-temperature transition at ~55 °C is present, again suggesting some complex disruption under these conditions. However, in these strongly reacting systems, we suspect that uniform accessibility of Ca^{2+} to all available binding sites may be difficult to achieve due to the formation of the collapsed, essentially dehydrated multibilayer complex. Thus, in some cases, we may be observing effects due to sample heterogeneity. As indicated by the experiments shown in Figure 4, these problems may be minimized by starting with sonicated bilayer dispersions to which Ca^{2+} is added. In this case, only the high-temperature transition is observed for DPPS in 0.5 M $CaCl_2$, although in this case the Ca^{2+}(total):DPPS ratio is also much higher (~50:1) than that discussed above.

The X-ray diffraction data recorded at 20 °C provide convincing evidence for a homologous series of Ca^{2+}–PS complexes. The series of strong diffraction lines in the wide-angle region suggest strongly that lateral intermolecular interactions induced by Ca^{2+} result in chain crystallization. The chain packing mode presumably corresponds to a complex hybrid subcell characteristic of phospholipids [see Elder et al. (1977), Abrahamsson et al. (1978), and Shipley (1984)] rather than the simpler chain packing modes associated with the simpler monoacyl lipids such as alkanes, fatty acids, etc. (Abrahamsson et al., 1978). For the Ca^{2+}–PS complexes, the bilayer periodicities correspond closely to those of the *anhydrous* type II PS structures (Hauser et al., 1982). This suggests that all the Ca^{2+}–PS complexes are essentially anhydrous and that the chains are tilted with respect to the bilayer normal as shown in Figure 8 (see also Mg^{2+}–DMPS and Mg^{2+}–DPPS). The precise location of the Ca^{2+} ion with respect to the PS bilayer and its coordination with respect to binding sites on the PS polar group remain to be established by high-resolution structural investigations.

It seems likely that similar high-melting, ordered bilayer phases are induced by calcium binding to bovine brain PS; however, it should be noted that Mg^{2+} appears to be far less effective at forming these types of complexes with bovine brain PS [see Papahadjopoulos et al. (1977, 1978), Jacobson & Papahadjopoulos (1975), and Newton et al. (1978)]. The different binding characteristics of Mg^{2+} with saturated PS and bovine brain PS may be due to the different molecular areas occupied at the lipid–water interface as dictated by the hydrocarbon chain composition. Presumably, Ca^{2+} binding is less sensitive with respect to the PS molecular area at the interface. Experiments with synthetic PS containing unsaturated fatty acids have been designed to test this hypothesis (H. Hauser and G. G. Shipley, unpublished results).

Sr^{2+}- and Ba^{2+}–PS Complexes. The calorimetric data show that for DPPS, at least, 50 molar excess concentrations of Sr^{2+} and Ba^{2+} produce a behavior different from that induced by Mg^{2+} and Ca^{2+}. With sonicated DPPS, addition of Sr^{2+} or Ba^{2+} shifts the transition temperature to 71 or 79 °C, respectively, and some complex melting behavior is observed in the range 150–190 °C. When examined by X-ray diffraction at 20 °C, the Sr^{2+}–DPPS and Ba^{2+}–DPPS complexes show little evidence of hydrocarbon chain crystallization. For Sr^{2+}–DPPS, only a single wide-angle reflection at $1/4.2$ Å^{-1} is present, an indication of the usual hexagonal chain packing mode characteristic of gel-state phospholipids. Some, albeit weak, additional lines are observed for Ba^{2+}–DPPS, perhaps indicating some formation of a more ordered complex, but the dominant reflection is again at $1/4.2$ Å^{-1}. Although Sr^{2+} and Ba^{2+} appear to have little effect on the lateral molecular packing, they do induce bilayer condensation or collapse similar to that induced by Mg^{2+} and Ca^{2+}. Thus, the bilayer periodicity for both complexes is 58 Å, a value corresponding to that of the nontilted *anhydrous* form I PS. Thus, bilayer dehydration without chain crystallization is apparently induced by Sr^{2+} and Ba^{2+} (see Figure 8).

Conclusions

Our previous studies have shown that monovalent cations such as Na^+ and K^+ have little effect on PS bilayer structure, stability, and chain packing (Hauser & Shipley, 1983). Their dominant effect is in shielding the negatively charged surface and allowing an ionic strength dependent reduction in the aqueous separation of adjacent bilayers. In contrast, the monovalent cation Li^+ [see Hauser & Shipley (1981, 1983)] and the divalent cations Mg^{2+} and Ca^{2+} (this study), all with small ionic radii, form strong, essentially dehydrated complexes with PS (Figure 8). For DPPS, for example, these complexes exhibit chain melting transitions at high temperatures, approximately 95 °C for Li^+ and Mg^{2+} and 155 °C for Ca^{2+}. The Mg^{2+} and Ca^{2+} complexes, at least of DMPS and DPPS, appear to be structurally similar with tilted chain arrangements, whereas the Li^+ complex has a nontilted structure (see Figure 8). The larger divalent cations Sr^{2+} and Ba^{2+}, while inducing bilayer dehydration and stacking, do not as readily form the high-melting complexes. Given the differential ability of the divalent cations to induce bilayer fusion, we might argue that the *combined* effect of local bilayer dehydration *and* bilayer chain crystallization as elicited by Ca^{2+} and Mg^{2+} (and not Sr^{2+} and Ba^{2+}) is of importance in this discriminatory effect.

Registry No. Mg, 7439-95-4; Ca, 7440-70-2; Sr, 7440-24-6; Ba, 7440-39-3; Li, 7439-93-2; DDPS, 80581-67-5; DLPS, 76260-76-9; DMPS, 64023-32-1; DPPS, 40290-42-4; DSPS, 51446-62-9; DPPS·NH_3, 80538-62-1.

References

Abrahamsson, S., Dahlen, B., Lofgren, H., & Pascher, I. (1978) *Prog. Chem. Fats Other Lipids 16*, 125–143.

Abramson, M. B., Katzman, R., & Gregor, H. P. (1964) *J. Biol. Chem. 239*, 70–76.

Atkinson, D., Hauser, H., Shipley, G. G., & Stubbs, J. M. (1974) *Biochim. Biophys. Acta 339*, 10–29.

Browning, J. L., & Seelig, J. (1980) *Biochemistry 19*, 1262–1270.

Cevc, G., Watts, A., & Marsh, D. (1981) *Biochemistry 20*, 4955–4965.

Eisenberg, M., Gresalfi, T., Riccio, T., & McLaughlin, S. (1979) *Biochemistry 18*, 5213–5223.

Elder, M., Hitchcock, P., Mason, R., & Shipley, G. G. (1977) *Proc. R. Soc. London, Ser. A 354*, 157–170.

Elliott, A. J. (1965) *J. Sci. Instrum. 42*, 312–316.

Hauser, H., & Phillips, M. C. (1973) *J. Biol. Chem. 248*, 8585–8591.

Hauser, H., & Shipley, G. G. (1981) *J. Biol. Chem. 256*, 11377–11380.

Hauser, H., & Shipley, G. G. (1983) *Biochemistry 22*, 2171–2178.

Hauser, H., Finer, E. G., & Darke, A. (1977) *Biochem. Biophys. Res. Commun. 76*, 267–274.

Hauser, H., Pascher, I., Pearson, R. H., & Sundell, S. (1981) *Biochim. Biophys. Acta 650*, 21–51.

Hauser, H., Paltauf, F., & Shipley, G. G. (1982) *Biochemistry 21*, 1061–1067.

Hermetter, A., Paltauf, F., & Hauser, H. (1982) *Chem. Phys. Lipids 30*, 35–45.

Hope, M. J., & Cullis, P. R. (1980) *Biochem. Biophys. Res. Commun. 92*, 846–852.

Jacobson, K., & Papahadjopoulos, D. (1975) *Biochemistry 14*, 152–161.

Loosley-Millman, M. E., Rand, R. P., & Parsegian, V. A. (1982) *Biophys. J. 40*, 221–232.

Luna, E., & McConnell, H. M. (1977) *Biochim. Biophys. Acta 470*, 303–316.

MacDonald, R. C., Simon, S. A., & Baer, E. (1976) *Biochemistry 15*, 885–891.

McLaughlin, A. C. (1982) *Biochemistry 21*, 4879–4885.

McLaughlin, S., Mulrine, N., Gresalfi, T., Vaio, G., & McLaughlin, A. (1981) *J. Gen. Physiol. 77*, 445–473.

Newton, C., Pangborn, W., Nir, S., & Papahadjopoulos, D. (1978) *Biochim. Biophys. Acta 506*, 281–287.

Ohki, S., & Kurland, R. (1981) *Biochim. Biophys. Acta 645*, 170–176.

Ohki, S., Duzgunes, N., & Leonards, K. (1982) *Biochemistry 21*, 2127–2133.

Ohnishi, S., & Ito, T. (1974) *Biochemistry 13*, 881–887.

Papahadjopoulos, D. (1978) *Cell Surf. Rev. 5*, 765–790.

Papahadjopoulos, D., & Hanahan, D. J. (1964) *Biochim. Biophys. Acta 90*, 436–439.

Papahadjopoulos, D., & Miller, N. (1967) *Biochim. Biophys. Acta 135*, 624–638.

Papahadjopoulos, D., Vail, W. J., Newton, C., Nir, S., Jacobson, K., Poste, G., & Lazo, R. (1977) *Biochim. Biophys. Acta 465*, 579–598.

Papahadjopoulos, D., Portis, A., & Pangborn, W. (1978) *Ann. N.Y. Acad. Sci. 308*, 50–63.

Puskin, J. S. (1977) *J. Membr. Biol. 35*, 39–55.

Rouser, G., Nelson, G. J., Fleischer, S., & Simon, G. (1968) *Biol. Membr. 1*, 5–69.

Schick, P. K., Kurica, K. B., & Chacko, G. K. (1976) *J. Clin. Invest. 57*, 1221–1226.

Shipley, G. G. (1984) in *The Physical-Chemical Behavior of Lipids* (Small, D. M., Ed.) Plenum Press, New York (in press).

Smith, H. G., Fager, R. S., & Litman, B. J. (1977) *Biochemistry 16*, 1399–1405.

van Dijck, P. W. M., de Kruijff, B., Verkleij, A. J., van Deenen, L. L. M., & de Gier, J. (1978) *Biochim. Biophys. Acta 512*, 84–96.

Verkleij, A. J., Zwaal, R. F. A., Roelofsen, B., Confurius, P., Kastelijn, D., & van Deenen, L. L. M. (1973) *Biochim. Biophys. Acta 323*, 178–193.

White, D. A. (1973) *BBA Libr. 3*, 441–482.